Medicinal Chemistry Research (2020) 29:377–395
https://doi.org/10.1007/s00044-019-02487-2

MEDICINAL CHEMISTRY RESEARCH

ORIGINAL RESEARCH

Styrylcoumarin 7-SC2 induces apoptosis in SW480 human colon adenocarcinoma cells and inhibits azoxymethane-induced aberrant crypt foci formation in BALB/c mice

Angie Herrera-R[1,2] · Tonny W. Naranjo[3,4] · Maria Elena Maldonado[2] · Gustavo Moreno-Q[1] · Andrés Yepes[1] · Wilson Cardona-G[1]

Received: 25 June 2019 / Accepted: 28 November 2019 / Published online: 9 December 2019

Abstract

In vivo chemopreventive effects associated with hybrid molecules against colon carcinogenesis remain poorly studied. In a previous study, we showed that styrylcoumarin hybrids **3-SC1**, **7-SC2** (2,7-(4-hydroxy-3,5-dimethoxystyryl)-coumarin), and **7-SC3** decrease cell viability of SW480 in a time- and concentration-dependent manner ($IC_{50\text{-}SW480/48\,h} = 6.92$; 1.01 and 5.33 μM, respectively) with high selectivity indices after 48 h of treatment (>400; 67.8 and 7.2, respectively). The present study investigates the mechanisms of these three styrylcoumarins to induce cell death, using an in vitro model of colon adenocarcinoma cells (SW480); besides, it evaluates anticarcinogenic properties in vivo for the most active molecule. According to the results, none of the hybrids exhibited significant changes in cell cycle distribution of SW480 cells with respect to control group ($G_0/G_1 = 85.5\%$, $S = 7.2\%$, and G_2/M 7.3%), which indicates that these do not have a cytostatic effect on this cell line. Besides, they did not cause mitochondrial depolarization, suggesting an alternative source for the production of reactive oxygen species (ROS). Among the evaluated compounds, the most active molecule **7-SC2** induced a greater production of ROS in comparison with the control ($p < 0.05$) together with a significant increase in the expression of p53, caspase-3, and a significant reduction in the production of interleukin-6 of SW480 cells. When colon carcinogenesis was induced in Balb/c mice by intraperitoneal injections of azoxymethane, a significant reduction ($p < 0.05$) in the number of preneoplastic lesions of mice treated with styrylcoumarin hybrid **7-SC2** was observed with regard to the control group. In addition, no side effects were associated with the administration of the compound. All these in vitro results and the effective reduction of preneoplastic lesions in vivo suggest that styrylcoumarin **7-SC2** induces apoptosis in primary tumor cells and implies the potential ability at the early post-initiation phases of colon carcinogenesis. Moreover, hybrid **7-SC2** was docked to the three-dimensional structures of different apoptotic proteins and inflammatory cytokines, showing high binding affinities (ranging from −10.0 to −7.2 kcal/mol). Good correlation between calculated binding energies and experimental results was obtained. According to in silico ADME (absorption, distribution, metabolism, and excretion) studies of the **7-SC2**, this novel compound has suitable drug-like properties, making it a potentially promising agent for therapy against colon cancer.

Keywords Styrylcoumarin · Cell death · Aberrant crypt foci · Colorectal cancer · In silico studies

✉ Angie Herrera-R
angie.herrerar@udea.edu.co

✉ Wilson Cardona-G
wilson.cardona1@udea.edu.co

[1] Química de Plantas Colombianas, Institute of Chemistry, Faculty of Exact and Natural Sciences, University of Antioquia, UdeA, Calle 70 No. 52-21, A.A 1226 Medellín, Colombia

[2] Grupo Impacto de los Componentes Alimentarios en la Salud, School of Dietetics and Nutrition, University of Antioquia, A.A. 1226 Medellín, Colombia

[3] Grupo de Micología Médica y Experimental, Corporación para Investigaciones Biológicas, Medellín, Colombia

[4] School of Health Sciences, Universidad Pontificia Bolivariana, Medellín, Colombia

Abbreviations

CRC	Colorectal cancer
ACF	Aberrant crypt foci
AOM	Azoxymethane
SS	Saline solution
DMSO	Dimethylsulfoxide
APTES	(3-Aminopropyl)triethoxysilane

Introduction

Despite the fact that colorectal cancer (CRC) can be highly preventable through changes in lifestyle (Anand et al. 2008), this is still a leading cancer-related cause of death worldwide, being the second most common accounting for 881,000 deaths in 2018, only preceded by lung cancer, with an estimated 1.8 million new cases in the same year (Globocan 2018). Among the risk factors that contribute to CRC development, it is possible to include alcohol consumption, smoking, physical inactivity, obesity, diets high in fat and red meats, and inadequate intake of dietary fiber, vegetables, and fruits. Due to the widespread occurrence of the risk factors and the increase in the statistics, extensive research is ongoing to develop new pharmaceutical agents with chemopreventive potential against CRC. The pathogenesis of CRC comprises a multistep process with deregulation of epithelial cells into a polyp, which may evolve to a cancerous state. Aberrant crypt foci (ACF) were first identified as putative precancerous lesions in the colon of carcinogen-treated rodents (Alrawi et al. 2006), and it is well known that there are similar genotypic and morphological characterizations of ACF between animal and human colons. These structures are microscopically characterized by crypts with elevated sizes above the normal mucosa composed of thickened luminal epithelia, easily discernible pericryptal zones (Bird and Good 2000), and they are extensively used as a biomarker in the early stages of pathogenesis of colon cancer to investigate the effects of potential chemopreventive agents (Rouhollahi et al. 2015).

Current treatments for CRC include combinations of chemotherapeutic agents such as FOLFIRI (folic acid/5-fluorouracil (5-FU)/irinotecan) and FOLFOX (5-FU/leucovorin/oxaliplatin), which are composed of 5-FU as the backbone of the treatment, that, although effective, cause undesirable neurological and gastrointestinal side effects, which many times result in dose limitations or cessation of the anticancer therapy (Pointet and Taieb 2017; McQuade et al. 2014). Among the studies carried out in the search for cancer treatment, the use of hybrid molecules has been reported as a promissory strategy (Meunier 2008), since these molecules may display a dual mode of action, making them more efficient drugs (Shaveta and Singh 2016; Tsogoeva 2010). On this matter, a series of stilbene–coumarin hybrids were evaluated and authors found excellent antiproliferative potency and ability to induce apoptosis against lung carcinoma H460 (Belluti et al. 2010). On the other hand, another hybrid of styrylcoumarin was evaluated against breast (MCF-7) and colorectal (HCT-28) cancer cells, displaying growth inhibition on these two cell lines (Shen et al. 2013). Furthermore, a 3-phenylcoumarin with antiproliferative activity against promyeloblastic (HL-60) and lung carcinoma (A549) cell lines (Yang et al. 2011) was tested. Similarly, a benzimidazole–coumarin hybrid was screened in order to find in vitro antitumor activity on different cell lines; it was found that this molecule induced more than 50% inhibition of most of the cell lines evaluated, with higher selectivity against leukemic cancer cell lines (Paul et al. 2013). In addition, a coumarin–chalcone hybrid was evaluated against cervix carcinoma cells C33A and normal fibroblast NIH3T3, exhibiting great activity and selectivity at low concentrations (Sashidhara et al. 2010). Furthermore, a resveratrol–imidazole hybrid was evaluated against leukemia and renal cancer cell lines, showing high cytotoxic activity (Bellina et al. 2015). Finally, a resveratrol–chalcone conjugate was tested in ovarian cancer, non-small-cell lung cancer, and breast cancer cell lines, and the results indicated that this compound was highly active and selective (Kumar et al. 2014).

Similarly, animal studies have been conducted to determine the in vivo antitumor activity of hybrid compounds. Several resveratrol–caffeic acid hybrids were synthesized and evaluated in Kunming mice. Authors found that one compound significantly inhibited tumor growth when it was administered by oral route; besides, the hybrid molecule exhibited better safety than that found for chemotherapy medication, such as doxorubicin (Li et al. 2016). On the other hand, a series of benzopyran dihydropyrimidinone hybrids were evaluated in a mouse model of Ehrlich solid tumor, and the results showed tumor growth inhibition of these hybrids at a dose of 30 mg/kg/body weight (Dash et al. 2018). Finally, a new [1,3,5]-triazine–pyridine–biheteroaryl produced a significant survival increase when it was administered intraperitoneally at 150 and 125 mg/kg to nude mice bearing human A375 xenografts (Kuo et al. 2005).

In the above context, our laboratory recently identified several stilbene–coumarin hybrids "styrylcoumarins" (Fig. 1) endowed with in vitro activity against SW480 human adenocarcinoma colon cells. Among the evaluated compounds, hybrids **3-SC1**, **7-SC2** (2, 7-(4-hydroxy-3,5-dimethoxystyryl)-coumarin), and **7-SC3** exhibited the highest cytotoxic activity and selectivity (Herrera-R et al. 2018). In order to have an approach to the possible mechanism of action of the most active and selective compounds, we carried out some in vitro experiments to

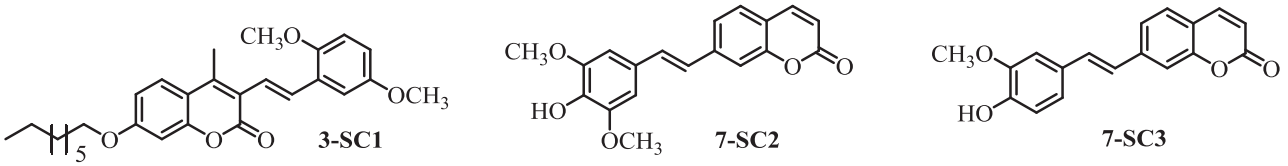

Fig. 1 Chemical structure of styrylcoumarins endowed with activity against SW480 cells

determine the effect on cell cycle, mitochondrial permeability, ROS production, apoptotic proteins, and inflammation-related biomarkers. Subsequently, the compound with the highest in vitro activity (**7-SC2**) was tested in vivo to know its effect at the early stage of carcinogenesis using an animal model for colon cancer.

Materials and methods

Source of the hybrid molecules

All compounds were synthesized by the group "Química de Plantas Colombianas," Faculty of Exact and Natural Sciences from the University of Antioquia (Medellín, Colombia). These were characterized by spectroscopic techniques as nuclear magnetic resonance and high-resolution mass spectra. The synthesis and cytotoxic activity of these hybrids was previously reported (Herrera-R et al. 2018).

In vitro biological assays

Cell line and culture medium

SW480 cells were obtained from The European Collection of Authenticated Cell Cultures (ECACC, England) in March 2017. According to the certification analysis from ECACC (Test number: 55133 fro; test date: November/December 2015), these were tested by cell count, viability, and confluency of cells on resuscitation from freezing. In addition, a test for the detection of mycoplasma by PCR, using mycoplasma-specific primers, was validated by ECACC, together with a test using a Vero indicator cell line Hoechst 33258 Fluorescent Detection System. Besides, the authentication of human cell lines by STR profiling using the PowerPlex® 16 HS PCR amplification kit was performed. A final sterility testing of cell banks was carried out for this human cell line. Cells were cultured in 25-cm^2 Falcon flasks containing Dulbecco's modified Eagle's medium, supplemented with 10% heat-inactivated (56 °C) horse serum, 1% penicillin/streptomycin, and 1% non-essential amino acids (Gibco Invitrogen, Carlsbad, USA). Cells were incubated at 37 °C in a humidified atmosphere of 5% CO_2. For all experiments, horse serum was reduced to 3%, and the medium was supplemented with 5 mg/ml transferrin, 5 ng/ml selenium, and 10 mg/ml insulin (ITS-defined medium; Gibco, Invitrogen, Carlsbad, USA) (Herrera-R et al. 2018; Massagué 2004; Pérez et al. 2014). In all experiments, cells were treated for 48 h since this was the optimal time in the previous study for cytotoxicity and selectivity (Herrera-R et al. 2018).

Effect of styrylcoumarins on cell cycle

Cell cycle distribution was analyzed by labeling cells with propidium iodide (PI). In brief, cells were seeded in six-well tissue culture plate at a density of 2.5×10^5 cells/ml, and then incubated at 37 °C in a 5% CO_2 atmosphere. The cultures were allowed to grow for 24 h and then were treated for 48 h with either 0.5% dimethylsulfoxide (DMSO) (vehicle control) or styrylcoumarin hybrids **3-SC1**, **7-SC2**, and **7-SC3**, with their respective half-maximal inhibitory concentration (IC_{50}) (6.92, 1.01, and 5.33 µM, respectively). After treatment, cells were scraped from the surface and the centrifuged cell pellet was resuspended with phosphate-buffered saline (PBS). Cell suspension was fixed in 1.8 ml of 70% ethanol at 4 °C overnight. The next day, cells were centrifuged, washed twice in PBS, and resuspended in 200 µl of PBS containing 0.25 mg/ml RNAse (Type I-A, Sigma-Aldrich, Germany), and 0.1 mg/ml PI. After incubation in the dark at 37 °C for 30 min, the PI fluorescence of 10,000 cells was analyzed using a FACS Canto II flow cytometer and the BD FACS Diva 6.1.3 software (BD Biosciences, San Jose). Cell clumps were excluded with the signals on the forward scatter (FSC), using the FSC height (FSC-H) versus the FSC area at 488 nm. Cell cycle model was fixed using the FlowJo 7.6.2 software (Ashland, OR, USA) by applying the Dean–Jett–Fox model (García-Gutiérrez et al. 2017; Nicoletti et al. 1991).

Effect of styrylcoumarins on the mitochondrial membrane potential

Cells were seeded at a density of 2.5×10^5 cells/well in six-well tissue culture plates and allowed to grow for 24 h. Afterward, cells were treated for 48 h with either DMSO 0.5% (control) or styrylcoumarin hybrids **3-SC1**, **7-SC2**, and **7-SC3**, with their respective IC_{50} values (6.92, 1.01, and 5.33 µM, respectively). Cells were then harvested by scraping and stained with the fluorescent dye $DiOC_6$ (3,3′-

dihexyloxacarbocyanine iodide, Thermo Fisher Scientific, Waltham, MA, USA) and PI at 37 °C for 30 min in darkness. Cells were collected to analyze 10,000 events by flow cytometry with excitation at 488 nm and detection of the emission with the green (530/15 nm) and the red (780/60 nm) filters. This method allows quantifying cells with changes in the mitochondrial membrane permeability (García-Gutiérrez et al. 2017).

Determination of ROS

In order to evaluate if the treatment with the most active styrylcoumarin induces oxidative stress that could be related with mitochondrial damage, SW480 cells were seeded at a density of 2.5×10^5 cells/well in six-well tissue culture plates allowing them to grow for 24 h; afterward, these were treated for 48 h with either DMSO 0.5% (control) or styrylcoumarin hybrid **7-SC2**. CM-H2DCFDA (5-(and 6)-chloromethyl-2′,7′-dichlorodihydrofluorescein diacetate) was then added at a final concentration of 8 μM and incubated for 30 min at 37 °C. Analysis was made by flow cytometry. ROS production was expressed as percentage (%) increase in fluorescence relative to untreated control cells.

Determination of inflammatory cytokines and apoptotic proteins

SW480 cells were cultured and exposed to the most active styrylcoumarin **7-SC2**. After 48 h of treatment, cells were collected by scraping and lysed with Cell Lysis Buffer (1×, Ref. #9803). The supernatant was used to determine the effect of styrylcoumarin treatment on the modulation of inflammatory cytokine levels (IL-1β, IL-6, and tumor necrosis factor-α (TNFα)) and apoptotic proteins such as phospho-p53, p53, cleaved caspase-3, cleaved poly (ADP-ribose) polymerase (PARP), phospho-Bad, Bad (Pathscan® Apoptosis Multi-target Sandwich ELISA, Cell Signaling Technology), Bcl-2 (Cell Signaling Technology), and Bax (Elabscience Biotechnology Co., Ltd., China). The assays were performed according to the manufacturer's instructions.

In vivo assays

Animals

Male and female BALB/c mice (n:30), 10 weeks old, weighting 18–22 g were used; these were housed in the vivarium of "Corporación para Investigaciones Biológicas" under standardized conditions in a cage-level barrier system: 22–25 °C, 12-h light/12-h dark cycle, rodent diet, and free access to drinking water. All procedures were conducted in accordance to current national (Law 84/1989, resolution no. 8430/1993) and international guidelines (European Union: Directive 2010/63/EU and Canadian Council on Animal Care regulations). The protocol was approved on the 1st of July 2015 by the Institutional Ethics Committee.

In vivo experimental design

In the experimental design several groups were included as controls. The first group ($n = 6$) was named "ACF: Negative control" (G1) and received intraperitoneal injection of NaCl 0.9% once a week for 2 weeks. At the same time, one group of mice ($n = 18$) received intraperitoneal injection of azoxymethane (AOM) (Sigma-Aldrich), 10 mg/kg body weight, once a week for 2 weeks. One week after the last injection of AOM, these injected animals were randomly separated into three groups: "ACF: Positive control" (G2; $n = 6$; did not receive any treatment), "Vehicle control" (G3; $n = 6$; ethanol 5% v/v), and "Treatment" (G4; $n = 6$; styrylcoumarin **7-SC2** at a dose of 10 mg/kg body weight). A last group ($n = 6$) did not receive any injection, but it was also treated with the styrylcoumarin **7-SC2** alone, serving as "Treatment control" (G5) to evaluate possible side effects. All groups were kept under the same conditions. Treatments started 1 week after the second AOM injection and they were given by oral gavage thrice a week/8 weeks (Fig. 2) (Corrales-Bernal et al. 2016).

Histopathological analysis: assessment of aberrant crypts

All animals were killed 8 weeks after the last AOM or saline injection; the most distal part of the colon (4 cm in length) was washed with physiological saline, cut, opened, and placed onto a glass slide (APTES-treated glass slides were used to avoid tissue detachment). The segment was fixed in 10% buffered formalin for a minimum of 24 h and then stained with 0.2% methylene blue for 5 min, rinsed in Krebs-Ringer buffer, and examined microscopically using a low-power objective (×4) for the assessment of hyperproliferative aberrant crypts and ACF. The histomorphological criteria for the identification of hyperproliferative aberrant crypts were (i) an increased size, (ii) a thicker epithelial cell lining, and (iii) an increased pericryptal zone relative to normal crypts (Bousserouel et al. 2011).

Statistical analysis

All experiments were performed at least three times. Data are reported as mean ± SE (standard error). Statistical differences between control group (non-treated) and treated ones were evaluated by one-way analysis of variance followed by the Dunnett's test. Values with $p \leq 0.05$ were considered significant. Data were analyzed with GraphPad Prism version 7.04 for Windows (GraphPad Software, San Diego, CA, USA).

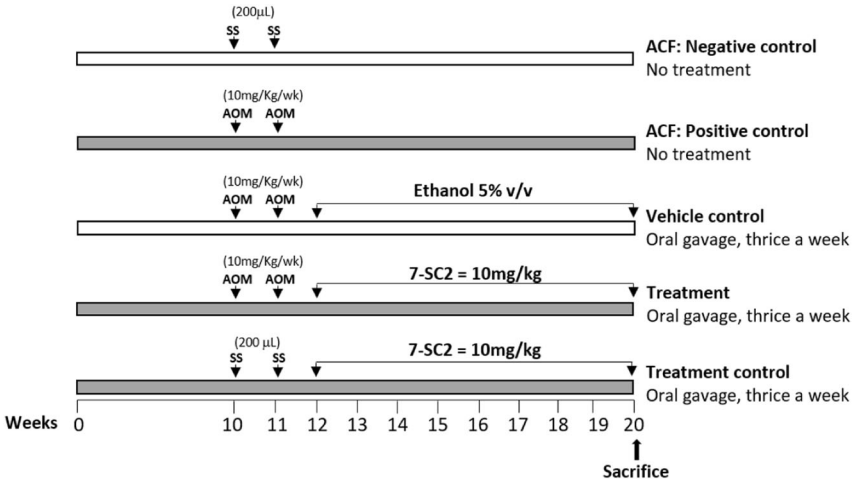

Fig. 2 Experimental procedure used for the AOM mouse model

Drug-likeness evaluation

In silico drug-likeness prediction along with further ADME tools present an array of opportunities to accelerate the discovery of new anticancer drugs. To find out the drug-like properties for styrylcoumarin **7-SC2**, the ADME physicochemical parameters were determined using open-source cheminformatics toolkits such as Molinspiration software (for MW, H-bond donors, H-bond acceptors, rotatable bonds, and TPSA descriptors). ALOGPS 2.1 algorithm from the Virtual Computational Chemistry Laboratory (for log $P_{o/w}$ and aqueous solubility log S_w descriptors) and PreADMET 2.0 were used to predict various pharmacokinetic parameters and pharmaceutical relevant properties such as apparent predicted intestinal permeability (App. Caco-2), binding to human serum albumin (K_{HSA}), Madin–Darby canine kidney (MDCK) cell permeation coefficients, and percentage human intestinal absorption (%HIA). These important parameters define absorption, permeability, movement, and action of drug molecules. The interpretation of two predicted ADME properties (MDCK and Caco-2 permeability) using PreADMET can be divided into three classes:

1. Permeability lower than 25: low permeability.
2. Permeability between 25 and 500: medium permeability.
3. Permeability higher than 500: high permeability.

Molecular-docking studies

Protein structure and setup

To explore the potential mechanism of action of styrylcoumarin **7-SC2**, different types of apoptotic proteins and pro-inflammatory cytokines were evaluated. The crystal structures of PARP (PDB: 4UND), mutant P53 (PDB: 1TSR-B), caspase-3 (PDB: 5I9B), MDM2 (PDB: 4HG7), Bcl-2 (PDB: 4MAN), BAX (PDB: 4S0O), VEGF (PDB: 1VPF), TNFα (PDB: 2AZ5), IL-6 (PDB: 1P9M), IL-1β (PDB: 2NVH), and COX-2 (PDB: 3LN1) were obtained from the Protein Data Bank. Initially, DNA, ligand, and crystallographic water molecules were removed in the three-dimensional structure using Discovery Studio Visualizer. For docking studies, the structures of the selected proteins and cytokines were parameterized using AutoDock Tools (Morris et al. 2009). In general, hydrogens were added to polar side chains to facilitate the formation of hydrogen bonds, and the Kollman and Gasteiger partial charges were calculated. AutoDock saved the prepared protein file in PDBQT format.

Ligand dataset preparation and optimization

In this study, the ligands included the novel styrylcoumarin **7-SC2** and four inhibitors that have been used as current drugs: celecoxib (COX-2), talazoparib (PARP), Nutlin-3a (MDM2), and a small-molecule inhibitor of TNFα. DS visualizer was used to rewrite the data files into pdb format. The structures of the ligands were parameterized using Autodock Tools to add full hydrogens to the ligands, to assign rotatable bonds, to compute Kollman and Gasteiger partial atomic charges, and to save the resulting structures in the required format to use with AutoDock. All possible flexible torsions of the ligand molecules were defined using AUTOTUTORS in AutoDock Tools (Morris et al. 2009, 1998) to facilitate the simulations of binding with the receptor structure.

Docking and posterior analysis

Docking simulations were performed with AutoDock 5.6 using the Lamarkian genetic algorithm and default procedures to dock a flexible ligand to a rigid protein. The

potential binding positions in all proteins were found using the reported active sites for each protein or calculated through Metapocket 2.0 server, which serves to identify the best binding pockets by predictive calculation of the topology of tertiary structures of selected subunits (Huang 2009). According to standard parameters, five binding pockets were calculated in the protein model and reliability of the model was assessed through the *Z*-value statistical test. Once potential binding sites were identified, docking of ligands to these sites was carried out to determine the most probable and most energetically favorable binding conformations. For these rigorous docking simulations involving a smaller search space (limited to the identified binding site), Autodock Vina was used (Trott and Olson 2010). The exhaustiveness (internal number of repetitions) was 20 for each protein–compound pair. The active site was surrounded by a docking grid of 30 $Å^3$ with a grid spacing of 1 Å. In addition, five replicates per compound were calculated to obtain the final docking score in kcal/mol. Docking solutions obtained through AutoDock Vina were ranked by the affinity scores, based on the free energy binding theory (more negative score indicates higher affinity). The resulting structures and some of the docked conformations were graphically inspected to check the interactions using DS visualizer or The PyMOL Molecular Graphics System, Version 2.0 Schrödinger, LLC.

Results and discussion

Chemoprevention is a strategy based on the use of natural, synthetic, or biological agents, which could reverse, suppress, or prevent either the initial phases of carcinogenesis or the progression of premalignant cells into invasive disease. This has markedly increased the interest in understanding the biology of carcinogenesis in order to identify molecular targets to disturb this process (Steward and Brown 2013; Russo 2007). According to this, the use of hybrid compounds has emerged as a promising strategy in medicinal chemistry and drug discovery research (Meunier 2008) since these molecules may display dual activity (Shaveta and Singh 2016; Tsogoeva 2010) and agents with different mechanisms of action is one of the methods adopted for treating cancer (Russo 2007; Kerru et al. 2017; Nepali et al. 2014; Mayur et al. 2009). The aim of the present study was to evaluate the effect of some styrylcoumarin hybrids in the immunomodulation and cell stability of human adenocarcinoma colon cells with respect to changes on cell cycle, mitochondrial membrane potential ($\Delta\Psi_m$), ROS production, apoptotic proteins, and inflammation-related biomarkers, as well as the effect in the formation of ACF during the early stage of carcinogenesis in a chemically induced colon cancer mouse model, since modulation in these processes are key hallmarks of colon cancer (Hanahan and Weinberg 2011; Shimizu et al. 2018). In a previous study, we found that styrylcoumarins **3-SC1**, **7-SC2**, and **7-SC3** displayed cytotoxic and antiproliferative effects on SW480 cells (Herrera-R et al. 2018). Here we made an approach to the mechanisms of these styrylcoumarins to induce cell death using an in vitro model of colon adenocarcinoma cells (SW480) and evaluated the most active molecule in an in vivo model of CRC in order to determine its chemopreventive activity.

Effect of styrylcoumarins on cell cycle distribution

The accumulation of mutations in tumor cells contributes to alterations in the cell cycle, which lead to inadequate proliferation of malignant cells (Massagué 2004). Thus, modulation of this event is seen as a possible target of action in the search of compounds with antitumor activity (Park and Lee 2003). Because of this, since hybrids **3-SC1**, **7-SC2**, and **7-SC3** exhibited the highest in vitro cytotoxic activity in a previous investigation that we conducted, with IC_{50} values of 6.92, 1.01, and 5.33 µM, respectively (Herrera-R et al. 2018), these were evaluated in order to determine the effect on cell cycle distribution of SW480 cells. They were treated with hybrid compounds during 48 h with their respective IC_{50}. Figure 3 shows the different peaks for each phase of the cycle distribution of SW480 after treatments. The highest peak represents the cells in G_0/G_1; the middle region exhibits the population in S phase of the cycle and the final peak on the right represents the cells in G_2/M phase. All results were compared with the control group ($G_0/G_1 = 85.5\%$; $S = 7.2\%$; $G_2/M = 7.3\%$). According to the results, compound **3-SC1** slightly increased the number of cells in G_2/M (9.8%), with a decrease in G_0/G_1 (84.8%) and S (5.4%). Besides, compounds **7-SC2** and **7-SC3** caused a small increase in G_0/G_1 (88.0% and 88.4%, respectively), with a decrease in the S phase (5.3% and 3.8%, respectively). However, these results were not statistically different, and this suggests that the mechanism of these hybrids is not associated not only with a cytostatic effect in SW480 cells, but also with other processes.

Changes in $\Delta\Psi_m$ induced by styrylcoumarin hybrids

Mitochondria plays a pivotal role in apoptosis by serving as a convergent center of apoptotic signals for both intrinsic and extrinsic pathways; besides, the changes induced in the $\Delta\Psi_m$ alter the permeability of the outer membrane, causing the release of proteins from the intermembrane space, a process that is directly involved in the intrinsic apoptotic pathway (Sánchez and Arboleda 2008; Sithara et al. 2017). Thus, these structures are considered an important target for designing compounds with chemopreventive potential. For

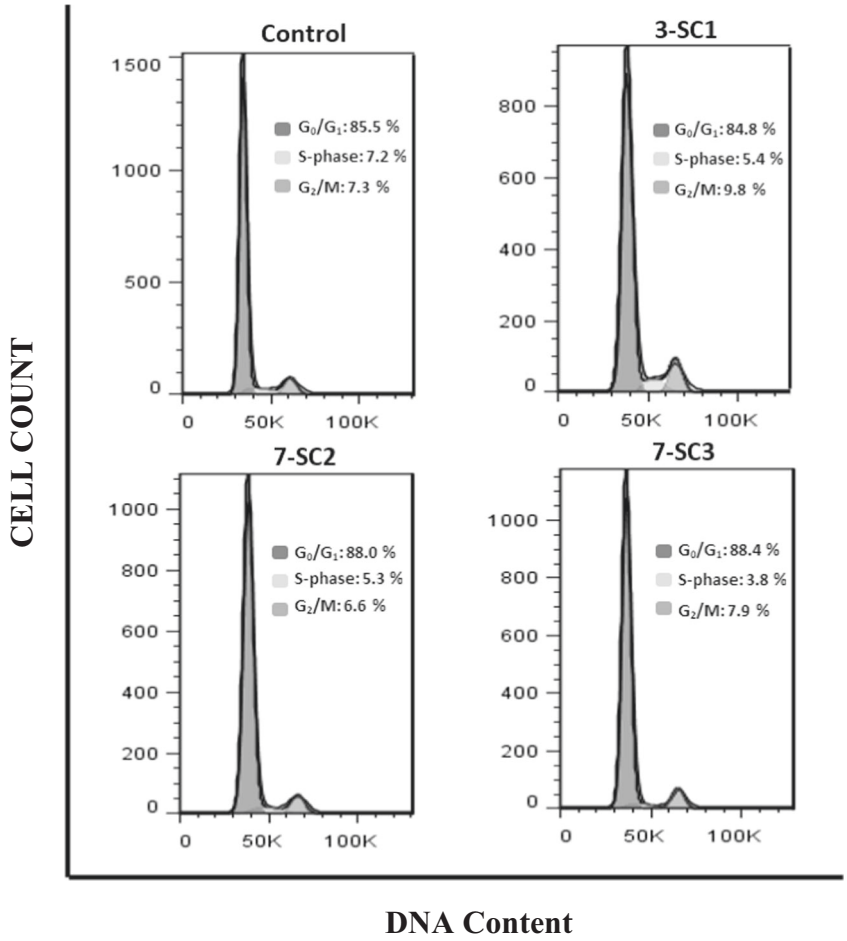

Fig. 3 Effect of styrylcoumarins on cell cycle of SW480 cells. The histograms represent one of three independent experiments. No statistical difference was observed between control group and treatments

this reason, we evaluated hybrids **3-SC1**, **7-SC2**, and **7-SC3** in order to determine the ability of these compounds to induce changes in the $\Delta\Psi_m$ that could cause mitochondrial dysfunction. After 48 h of treatment with the hybrids or DMSO 0.5% (control), SW480 cells were stained with the carbocyanine dye $DiOC_6$ and PI and analyzed by flow cytometry. $DiOC_6$ is a fluorescent dye that accumulates in mitochondria due to its large negative membrane potential and it is released to the cytosol after a membrane depolarization (membrane with reduced $\Delta\Psi_m$), staining intracellular membranes (García-Gutiérrez et al. 2017; Maldonado-Celis et al. 2008). Figure 4 shows the results for the $\Delta\Psi_m$. The right lower quadrant ($DIOC_6$ High) indicates the amount of live cells with high membrane polarization. The left lower region ($DiOC_6$ Low) and the upper quadrant indicate cells in latency that lose membrane polarization, with membrane damage and dead cells. According to the results, hybrid **7-SC3** was the only compound that caused a slight loss in mitochondrial membrane depolarization (0.974%) with regard to the control group (0.868%); however, these changes were not significant (Fig. 4a). In addition, it was observed that all hybrids evaluated (**3-SC1**, **7-SC2**, and **7-SC3**) significantly increased the population with positive staining for PI (8.51%, 14.1%, and 7.35%, respectively) (Fig. 4a). Cells in latency together with dead cells are clearly seen in Fig. 4b with their statistical significance. All these results suggest that the hybrids evaluated induce damage in cell membrane and death in SW480 cells in the conditions tested. Besides, since we did not observe mitochondrial dysfunction, this indicates that possibly the activation of the death signal is being triggered by an extrinsic pathway.

Determination of ROS

The production of radical oxygen species ROS in normal cells is an equilibrated event regulated by a variety of antioxidant defenses. When these molecules are produced in low doses, they play a role in physiological functions and they are essential for regulation of various cellular signaling pathways like cell cycle progression, proliferation, differentiation, migration, and cell death. However, when ROS production greatly exceeds the capacity of endogenous antioxidant systems, or when antioxidant levels are reduced, the excess of cellular levels of ROS increases, which is associated with induction of oxidative stress and signal

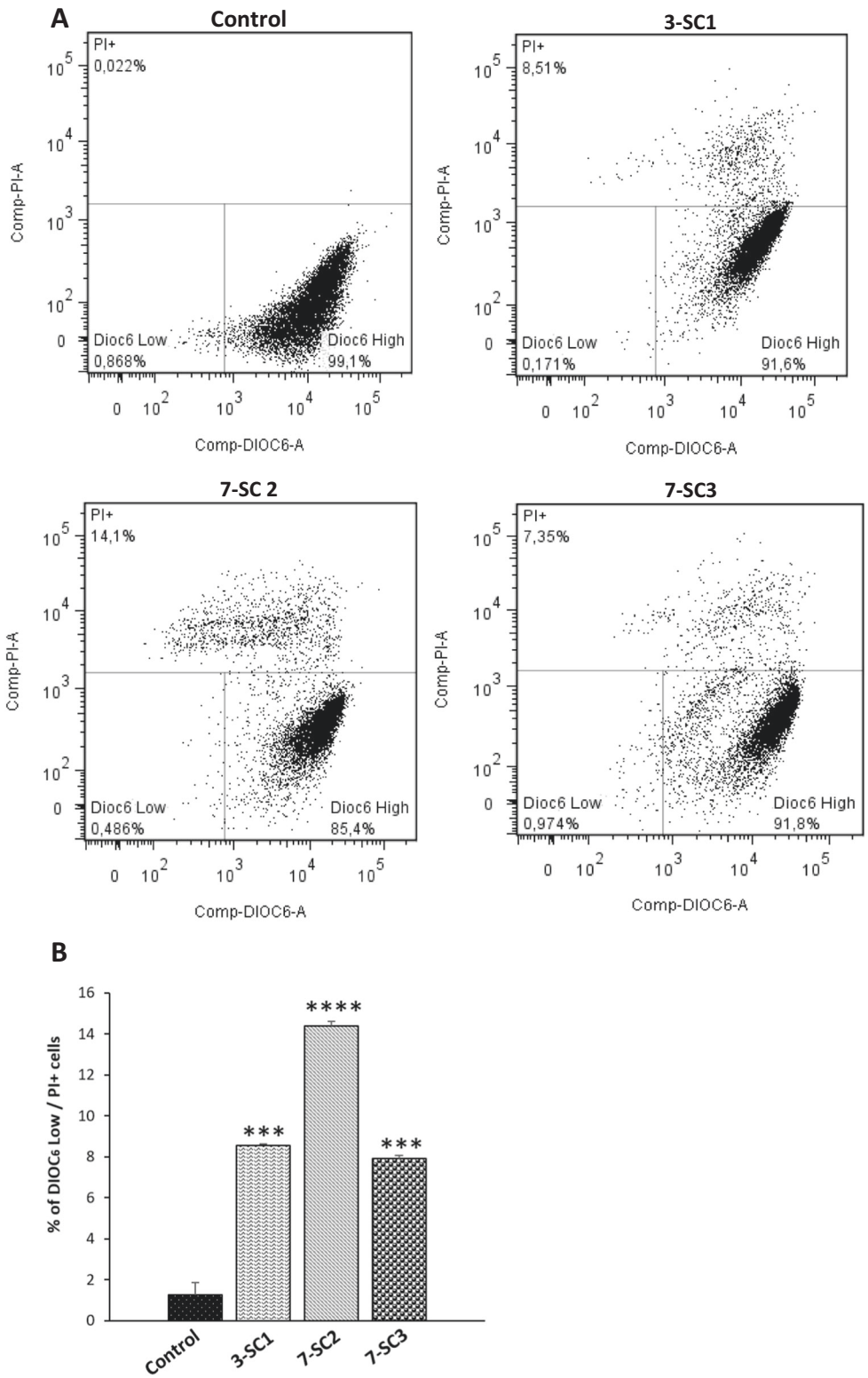

Fig. 4 Mitochondrial membrane potential in SW480 cells 48 h post treatment with styrylcoumarins or DMSO 0.5% (Control). **a** Flow cytometric analysis of cells stained with $DiOC_6$ and PI; $DiOC_6$ High: live cells with high membrane polarization; $DiOC_6$ Low and PI+: cells in latency that lose membrane polarization and dead cells. **b** Representation of data $DIOC_6$ Low and PI+ in bar chart form. Data are presented as the mean ± SE of three independent experiments. *p* Values lower than 0.05 were considered statistically significant (***$p < 0.001$; ****$p < 0.0001$)

transduction characterized by ROS-induced changes in cellular redox homeostasis, causing damage to proteins, nucleic acids, lipids, membranes, and organelles, which can lead to activation of cell death processes, such as apoptosis (Oparka et al. 2016; Gergely et al. 2002; Banki et al. 1999). The increase in ROS could be related to the accumulation and activation of p53 (Xie et al. 2001; Selivanova and Wiman 2007) through a mechanism that is not well defined (Xie et al. 2001). According to this, since hybrid **7-SC2** induced the highest damage to cells in the previous test with

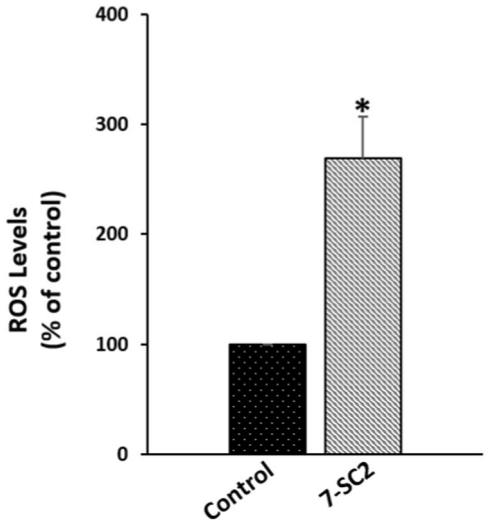

Fig. 5 Intracellular ROS induced by styrylcoumarin **7-SC2** or DMSO 0.5% (Control) in SW480 cells. Fluorescent dye CM-H2DCFDA was used. Data are presented as the mean ± SE of three independent experiments. p Values lower than 0.05 were considered statistically significant (*$p < 0.05$)

PI, at the lowest concentration, we evaluated it in order to determine if it induces oxidative stress that could be associated with mitochondrial damage. We used the indicator CM-H2DCFDA to know the effect in the production of radical oxygen species (ROS). The results obtained showed that this hybrid induced ROS formation in a greater proportion regarding the control; besides, these results were statistically significant with a p value lower than 0.05 (Fig. 5). On the other hand, since mitochondria is the main source of ROS and we did not observe changes in mitochondrial permeability, we suggest that possibly the activation of death signal is being triggered by the extrinsic pathway, enhanced by the production of ROS by other sources (Redza-Dutordoir and Averill-Bates 2016), as mentioned by Phaniendra et al. (2015) with regard to other ROS producers such as endoplasmic reticulum.

Effect of styrylcoumarin 7-SC2 on expression of apoptotic proteins

Considering that apoptosis is often impaired in many human tumors and it is also a significant event in chemotherapy, its modulation by targeting anti-apoptotic and pro-apoptotic proteins may be an important strategy for anticancer drug design, and the development of more selective apoptosis inducers is needed to reduce the side effects and increase efficacy. This process involves the sequential activation of proteases called caspases, some of them (effector caspases) are responsible for initiating the hallmarks of the degradation phase of apoptosis, including cell shrinkage, membrane blebbing, and DNA fragmentation (Brentnall et al. 2013). All these proteases are synthesized as proenzymes and require a highly regulated process to be activated, through cleavage (at specific aspartate residues) and dimerization (Park 2012). Caspases involved in apoptosis can be subclassified as initiator (caspase-8 and -9) or executioner caspases (caspase-3, -6, and -7) (Alotaibi et al. 2018). Once initiator caspases undergo self-activation, they can activate the executioner caspases to start the hydrolysis of different proteins from the cytoskeleton, nuclear proteins, and other molecules to initiate the final process of death (Park 2012). Among the executioner cysteine proteases, caspase-3 is one of the most important since it is the primary executioner of apoptotic death and cell decrease is more efficient in the presence of this protein (Brentnall et al. 2013); thus, we tested the effect of styrylcoumarin hybrid **7-SC2** on the levels of caspase-3 of SW480 cells after 48 h of treatment. We observed that this compound induced a significant increase in this protease, suggesting a mechanism of apoptosis in an in vitro model of CRC (Fig. 6a). Similar results were reported by Belluti et al. (2010). They found one stilbene–coumarin hybrid that induced activation of caspase-3 in human lung carcinoma H460, with detectable levels after 24 h of exposure, using concentrations between 1.5 and 3.0 μM.

In addition, the tumor-suppressor protein p53 has a pivotal role regulating different cellular processes such as apoptosis (Xie et al. 2001); thus, the effect of styrylcoumarin **7-SC2** was tested. Although this protein is mutated in SW480 cells, which results in an abnormal protein, it has been demonstrated that this molecule maintains residual DNA-binding ability and thus it retains some of the functions, being possible to activate it both in vitro and in vivo (Bykov and Wiman 2014) through different mechanisms that are still in study; for example, modifications at the N- and C-terminal domains (Selivanova and Wiman 2007). According to the results, we found that hybrid **7-SC2** induced the increase in the active form of p53 (Fig. 6a), despite the mutations, suggesting that this compound could change the conformational structure to restore the activity of this protein.

Likewise, we also evaluated the effect of styrylcoumarin **7SC-2** in the endogenous levels of Bad, phospho-Bad, cleaved PARP, Bcl-2 (Fig. 6a), and Bax (Fig. 6b), which are key molecules involved in the intrinsic apoptosis, since they control the mitochondrial permeability (Popgeorgiev et al. 2018). According to the results, the hybrid evaluated did not cause significant changes in those proteins, suggesting a different pathway in the apoptotic process, probably induced through the extrinsic route, not related with mitochondria, which is consistent with the previous assesment of ($\Delta\Psi_m$).

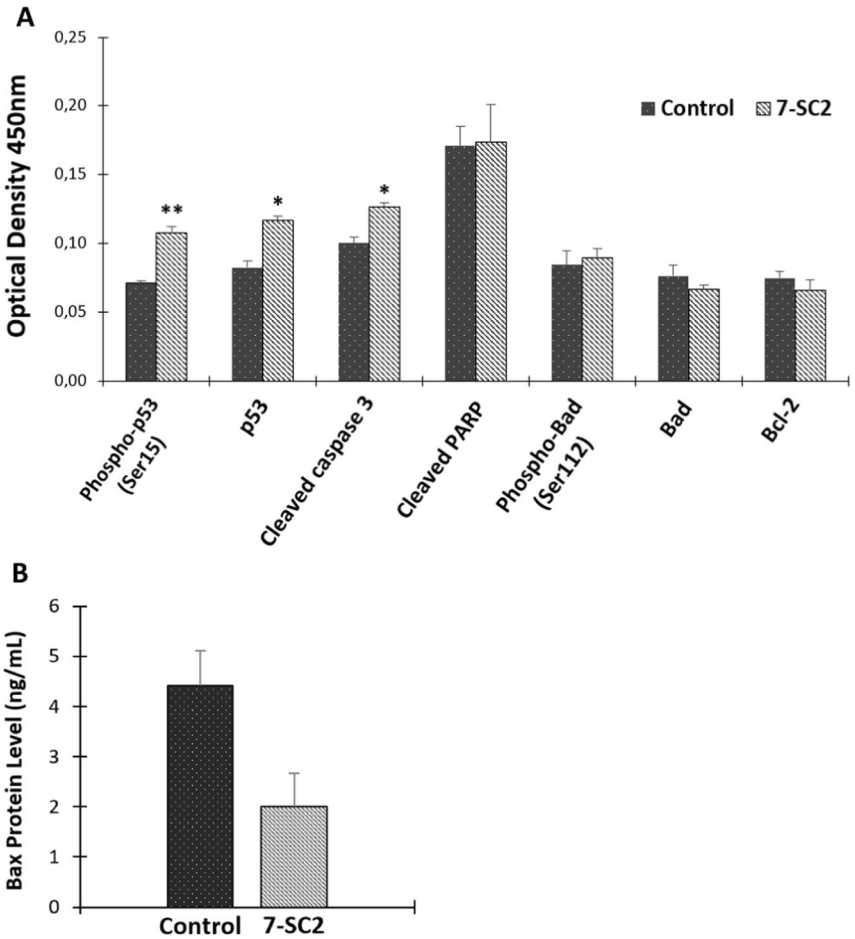

Fig. 6 Level of apoptotic biomarkers in SW480 cells 48 h post treatment with 1.01 µM of styrylcoumarin **7-SC2** or DMSO 0.5% (Control). **a** Level of p53, caspase-3, PARP, Bad, and Bcl-2 protein. **b** Level of pro-apoptotic Bax protein. Data are presented as the mean ± SE of three independent experiments (*$p < 0.05$; **$p < 0.01$). Optical density is directly proportional to the quantity of protein

Effect of styrylcoumarin 7-SC2 on expression of inflammatory cytokines

Regarding the inflammation role during carcinogenesis process, it has been widely observed that pro-inflammatory microenvironment can contribute directly to CRC development and progression. Several authors have reported, both in human and animal models, possible association between clinical, pathological, and pro-inflammatory cytokine levels such as IL-6, TNFα and IL-1β (Tanaka 2009); for this reason, downregulation of chronic inflammatory responses has been proposed as the effective strategy in chemoprevention. Different studies have reported an increase in the expression of IL-6 in patients with CRC; besides, authors mentioned that decreased levels in this cytokine prevent multiplicity and tumor progression in intestinal cells (Galizia et al. 2002; Knüpfer and Preiss 2009). Similarly, some studies have found association between high levels of TNFα with poor prognosis and progression of CRC (Sharma et al. 2008). This cytokine is used by tumor cells to evade immune response (Terzic et al. 2010). On the other hand, secretion of IL-1β in the tumor microenvironment increases the production of reactive oxygen and nitrogen species, which induce mutations in the colon, contributing to CRC development (Park and Lee 2003; Westbrook et al. 2009; Kauntz et al. 2012). After SW480 cells were treated with 1.01 µM of styrylcoumarin **7-SC2**, the levels of IL-6 were significantly lower with regard to control (Fig. 7); besides, we did not observe overexpression in TNFα and IL-1β, suggesting that the chemopreventive effect of this hybrid could be mediated by the regulation of cytokines as IL-6.

Effect of styrylcoumarin 7-SC2 on ACF formation

It is well known that excessive growth and inadequate apoptosis are often associated with development of intestinal tumorigenesis; besides, the early stage of colon cancer is characterized by a benign adenoma that could progress to adenocarcinoma with high-grade dysplasia (Chandrasekaran et al. 2018). On this matter, several spontaneous and chemically induced mouse models have been used to study experimental CRC since they exhibit many of the clinical, pathological, and molecular features occurring in sporadic human CRC (Chandrasekaran et al. 2018; Wargovich et al. 2010; Risio et al. 2010). There is an excellent

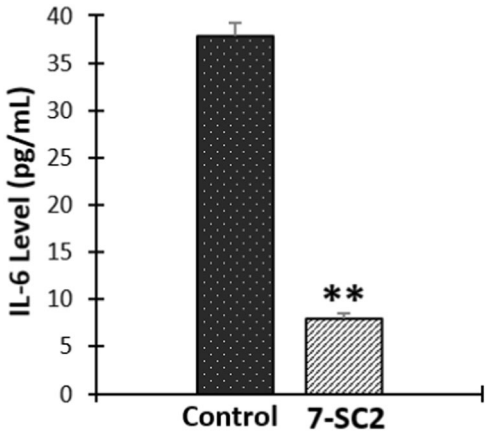

Fig. 7 Level of pro-inflammatory cytokine IL-6 in SW480 cells 48 h post treatment with 1.01 μM of styrylcoumarin **7-SC2** or DMSO 0.5% (control). Data are presented as the mean ± SE of three independent experiments (**$p < 0.01$). Optical density is directly proportional to the quantity of protein

experimental model chemically induced with AOM for studying CRC inflammation and pathogenesis. This model reproduces the multistep process of carcinogenesis characterized by the canonical phases of initiation, promotion, and progression (Chandrasekaran et al. 2018). Thus, the AOM model was used in order to get more insight into the chemopreventive potential of the most active styrylcoumarin hybrid **7-SC2** (Fig. 2). ACFs were used as biomarkers since they are the earliest histopathological manifestations of colon cancer (Wargovich et al. 2010), using the most distal part of the colon (Fig. 8a) to observe them. As shown in Fig. 8b–d, mice that were injected with AOM (FCA: positive control) experienced a great development of hyperproliferative crypts with higher size and reformed luminal epithelia, regarding normal control (FCA: negative control) and treatment group; besides, the number of aberrant crypts was statistically significant between them. The vehicle control group also exhibited a high amount of hyperproliferative crypts, which indicates that the effect of the styrylcoumarin hybrid **7-SC2** is not due to the reagent used to solubilize the molecule. Since the severity of the damage is also related to the number of crypts for each focus (Saki et al. 2017), it is interesting to note that none of the mice in the treatment group developed a focus with more than one crypt unlike the control groups ("ACF: positive control" and "vehicle control"). On the other hand, knowing that organ weight can be the most sensitive indicator of an effect of drug toxicity (Piao et al. 2013), it is important to highlight that the mean weight of organs such as heart, liver, kidneys, lungs, and spleen (Fig. 9a, b) from treated groups, was similar to the normal control, which suggests not apparent toxicity related with secondary effects after the treatment with styrylcoumarin **7-SC2** at the dose of 10 mg/kg/thrice a week; besides, none of the mice suffered from weight loss or died during the experiment, which suggests that these treatments were safe in the conditions evaluated. In addition, no statistical difference was found among female (Fig. 9a) or male mice (Fig. 9b). All these findings together with the results in the in vitro model suggest that this inhibition of the early stages of colon carcinogenesis could be related with antiproliferative or anti-inflammatory mechanisms; however, further studies need to be developed to elucidate the exact mode of action of this compound.

7-SC2 drug-likeness evaluation

We calculated and analyzed various drug-likeness properties for the most active compound **7-SC2** (Table 1). According to the results, hybrid **7-SC2** showed significant values for different parameters, exhibiting good drug-like characteristics, with values very similar for 95% of known drugs (or recommended ranges for an ideal drug). Regarding Lipinski's rule of five (Lipinski et al. 2001), this compound did not show violation of the rule that would make it a likely orally active drug in humans. In addition, it was observed that compound **7-SC2** exhibited high values of human intestinal absorption (% HIA) and 100% of human oral absorption (HOA %), which denote that this compound could be better absorbed from the intestinal tract upon oral administration. These in silico ADME predictions suggest that compound **7-SC2** follows the criteria for orally active drugs and thus it represents a pharmacologically active framework that should be considered on progressing further potential hits.

Applicability of these physicochemical properties is used to model many processes such as passive membrane permeation, where the molecular mechanism is hardly delineated. In this regard, Molecular Polar Surface Area (PSA), a descriptor that was shown to correlate well with passive molecular transport through membranes and allows prediction of drug–membrane interactions, was calculated. According to the results, the PSA value for **7-SC2** suggests that this compound tends to have a great affinity and good ability to penetrate through the tumoral cell (Ertl et al. 2000). Moreover, considering that lipophilicity is an important characteristic that influences a number of physiological properties, including transport through lipid bilayer, and it provides information on other drug-like properties such as lipid solubility, receptor binding, tissue distribution, cellular uptake, metabolism, and bioavailability, the log p value is used to measure the lipophilicity of a compound and it is a good indicator of permeability across the cell wall (Yang and Hinner 2002). In this study, hybrid **7-SC2** exhibited a log p value lower than 5, suggesting good permeability and permeation across the cell membrane of tumoral cells. In addition, in this work we

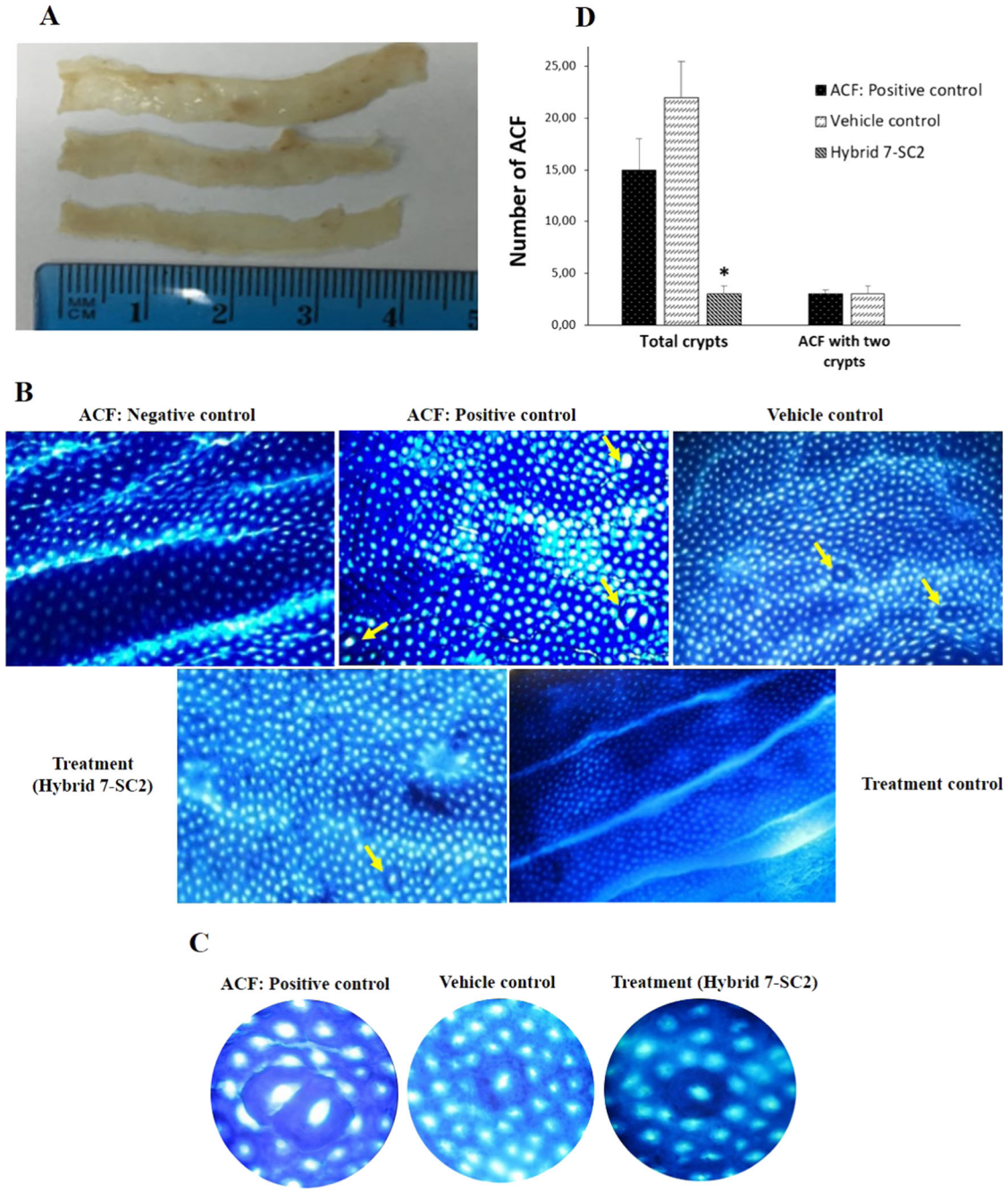

Fig. 8 Effect of hybrid **7-SC2** on ACF formation in the distal part of the colon from treated mice. **a** Representative image of distal colon from three different animals. **b** Colonic mucosa stained with methylene blue dye (magnification: ×10). Arrows indicate ACF localizations. **c** Hyperproliferative crypts and ACF at ×40 magnification. **d** Number of ACF. Data are presented as the mean (from six mice in each group ± SE). p Values lower than 0.05 were considered statistically significant (*$p < 0.05$)

calculated the number of rotatable bonds (n-rot), a simple topological parameter to measure molecular flexibility, and we found that the most active compound **7-SC2** contains six rotatable bonds, which gives the compound a high conformational flexibility, suggesting that it has a good absorption, results that correlate well with experimental findings where the compound reached a significant activity against CRC through in vitro and in vivo assays. On the other hand, in silico artificial membrane permeation in MDCK and Caco-2 was predicted for hybrid **7-SC2**. According to the results, this compound displayed high permeability values (529 and 1065 nm/s, respectively). In addition, the drug–plasma protein binding (K_{HSA}) was calculated for hybrid **7-SC2**, an early prediction that has vital importance in the characterization of drug distribution in the systemic circulation. Considering that unfavorable K_{HSA}

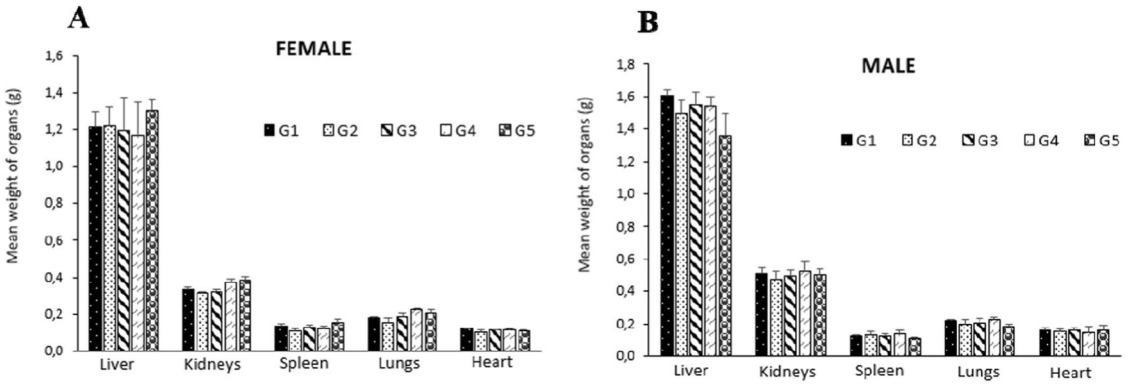

Fig. 9 Mean weight of organs from female (**a**) and male (**b**) mice. No statistical difference was found

Table 1 The physicochemical and drug-likeness evaluation for styrylcoumarin **7-SC2**

Properties	7-CS2
MW[a]	324.332
PSA[b] (7−200 Å^2)	73.710
n-Rot bond (<10)	6.0
n-ON[c] (<10)	4.75
n-OHNH[d] (<5)	1
Log $P_{o/w}$[e] (−2.0 to 6.5)	3.329
Log S_w[f] (−6.5 to 0.5)	−4.433
K_{HSA}[g] (% bound)	0.225
Caco-2[h] (nm/s) <25 poor; >500 great	1065
App. MDCK (nm/s)[i] <25 poor; >500 great	529
% HIA[j]	100
Lipinski's rule of five (≤1)	0
% HO[k] >80% is high <25% is low	High

[a]Molecular weight of the molecule

[b]Polar surface area (PSA) (7.0–200.0)

[c]n-ON number of hydrogen bond acceptors _10

[d]n-OHNH number of hydrogen bond donors ≤5

[e]Predicted octanol–water partition coefficient (log $P_{o/w}$) (−2.0 to 6.5)

[f]Aqueous solubility (Log S_w) (−6 to 0.5)

[g]In vitro binding constant to human serum albumin (K_{HSA})

[h]Predicted human intestinal permeability model (non-active gut–blood barrier transport; <25 poor; >500 great)

[i]Apparent permeability across cellular membranes of Madin–Darby canine kidney (MDCK) cells

[j]Human intestinal absorption (% HIA) (>80% is high; <25% is poor)

[k]Percent of human oral absorption (HOA %)

values can provide a negative effect on clinical development of a promising drug candidate for cancer treatment, it is possible to highlight that hybrid **7-SC2** was predicted at 100 percentage of binding. Finally, from the therapeutic point of view, the interpretation of predicted ADME properties showed values very similar for 95% of known drugs (or recommended ranges of an ideal drug), demonstrating the high potential of the **7-SC2** as a therapeutic candidate to design novel drugs for specific treatment of colon carcinogenesis.

Docking studies and prediction of binding pose

Computational docking refers to physical three-dimensional structural interactions that provide a means to predict and assess interactions between ligands (small molecules, proteins, peptides, etc.) and proteins (typically, proteins, DNA, RNA, etc.) (Horst et al. 2012). Docking methods are evaluated by predicting the correct pose/binding mode or by measuring predicted binding affinities. Considering the importance of apoptotic proteins and inflammatory cytokines in the carcinogenic process, we calculated the binding energy scoring function of **7-SC2** docked with different types of inflammatory cytokines and apoptotic proteins. The binding energy produced by docking action is tabulated in Table 2. According to the results, the highest negative energy value obtained after docking was found in hybrid **7-SC2** with PARP, with a docking score of −10, followed by COX-2 (−9.3 kcal/mol), mutant p53 (−9.1 kcal/mol), caspase-3 (−8.0 kcal/mol), MDM2, IL-6, and TNFα (−7.7 kcal/mol), Bcl-2 (−7.6 kcal/mol), VEGF (−7.4 kcal/mol), BAX (−7.2 kcal/mol), and IL-1β (−6.7 kcal/mol). In general, all proteins had high affinity and they are strongly bonded to polar contacts with the styrylcoumarin **7-SC2**, many of them comparable to current drugs. These results showed a strong correlation with the in vitro experimental assays, where a significant increase in the expression of the active form of p53, caspase-3, and a significant reduction in the production of IL-6 were observed in SW480 cells. Therefore, we rigorously examined the binding affinities of **7-SC2** on mutant p53, caspase-3, and IL-6.

Mutational inactivation of p53 is found in almost half of all human tumors; most of them are missense mutations occurring in the DNA-binding core domain of p53,

Table 2 Best binding energy (kcal/mol) based on AutoDock scoring of the styrylcoumarin **7-SC2**

Ligand	7-CS2	Celecoxib	Talazoparib	TNFα inhibitor	Nutlin-3a
Target protein docking score (kcal/mol)					
PARP	**−10**	–	−11	–	–
Mutant p53	**−9.1**	–	–	–	–
Caspase-3	**−8.0**	–	–	–	–
MDM2	−7.7	–	–	–	−7.7
Bcl-2	−7.6	–	–	–	–
BAX	−7.2	–	–	–	–
VEGF	−7.4	–	–	–	–
Interleukin-16	**−7.7**	–	–	–	–
Interleukin-1β	−6.7	–	–	–	–
TNFα	−7.7	–	–	−9.0	–
COX-2	−9.3	−9.2	–	–	–

Bold values indicate the best binding energy scores

PARP poly (ADP-ribose) polymerase, *MDM2* murine double minute 2, *Bcl-2* B-cell lymphoma-2, *BAX* Bcl-2-associated X protein, *VEGF* vascular endothelial growth factor, *TNFα* tumor necrosis factor-α, *COX-2* cyclooxygenase-2

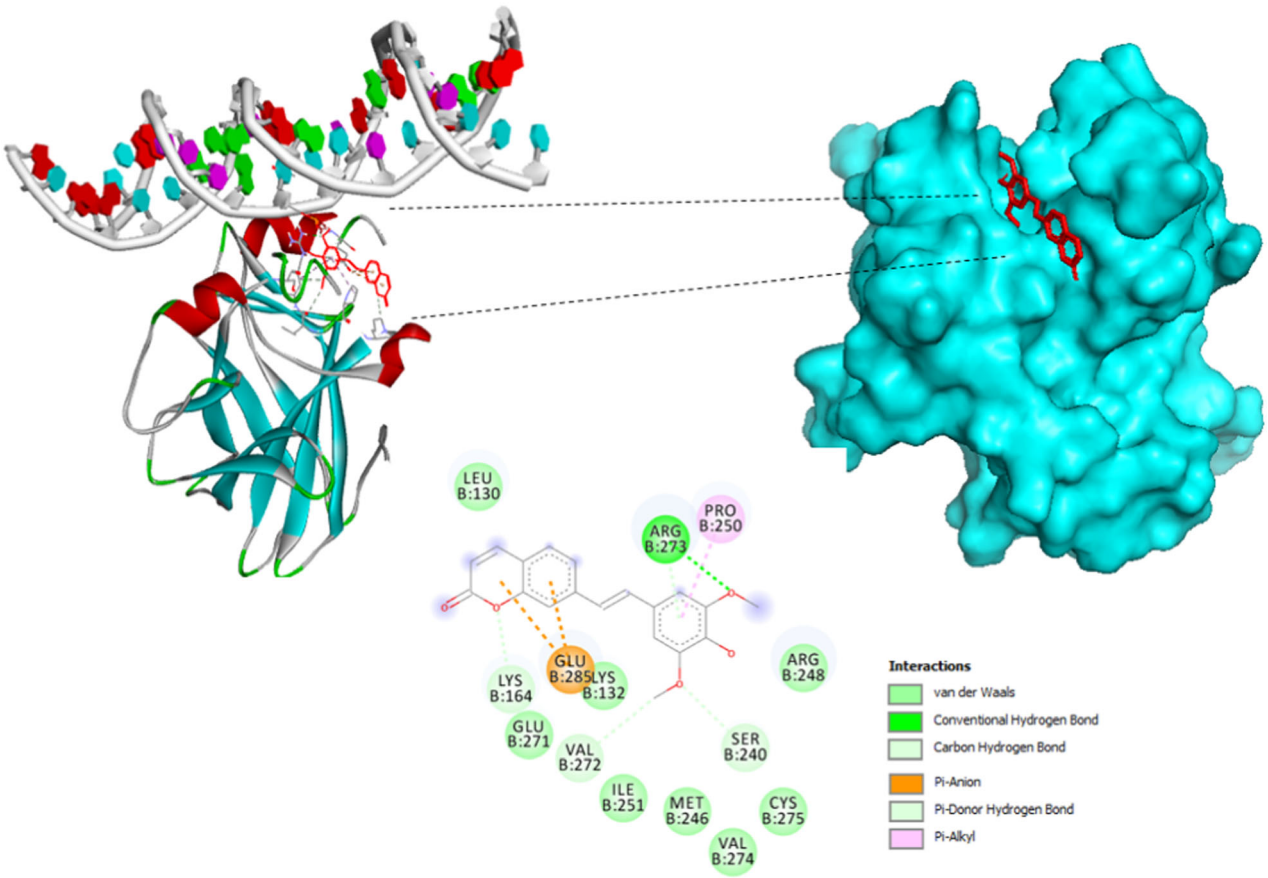

Fig. 10 The best docked ligand pose of hybrid **7-SC2** into the open L1/S3 pocket DNA-binding site of mutant p53 protein (PDB: 1TSR-B)

resulting in the disruption of protein–DNA interactions. Figure 10 shows the most stable binding pose of compound **7-SC2** (−9.1 kcal/mol), as suggested by the docking protocol in the DNA-binding site of mutant p53. Hybrid **7-SC2** was positioned between the L3 loop and H2 helix of p53 protein harboring DNA-contact residues. Malami et al.

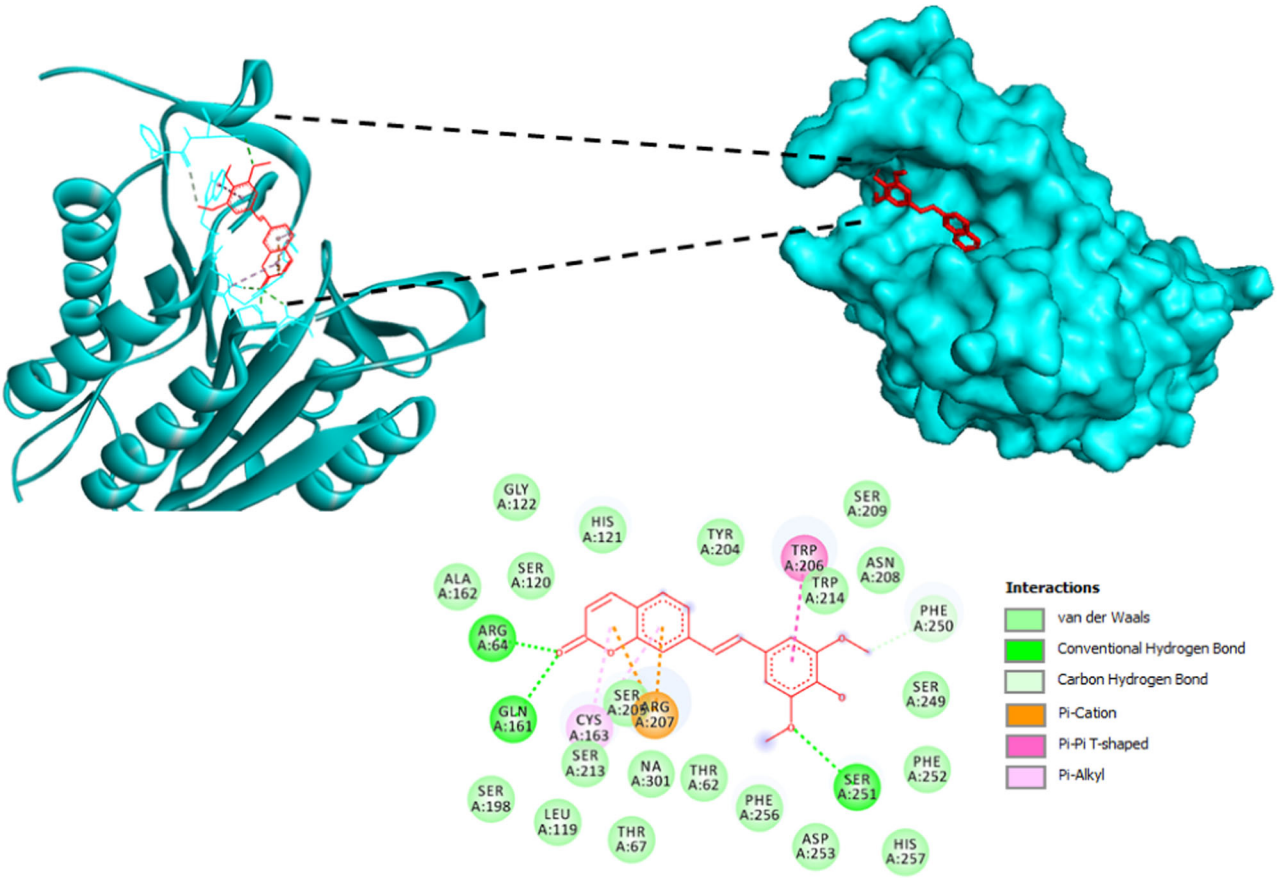

Fig. 11 The best conformation of **7-SC2** into the caspase-3 binding site

(2017) reported that the DNA-binding domain of mutant p53 is constituted by ARG273, ARG248, GLU285, PRO250, VAL272, LYS164, LYS132, SER241 and SER240. According to this, we found that styrylcoumarin **7-SC2** exhibits eight intermolecular interactions, in general, hydrophobic interactions that potentially confer stability during the binding event. Regarding these interactions of hybrid **7-SC2** with the DNA-binding domain of mutant p53, it was found that there was one hydrogen bond between a methoxy group and the ARG273 residue; two π–anion interactions between the aromatic coumarin ring and a carboxylic group of the GLU285 residue; π–sigma interactions between aromatic rings and the catalytic residues of PRO250 and LYS164. These in silico findings revealed that the molecular mechanism for **7-SC2** could involve restoration of wild-type p53 functional activity in tumor cells, which is correlated with our in vitro experimental results.

Caspases are a family of cysteine proteases associated with the induction of apoptosis (Van Opdenbosch and Lamkanfi 2019). Since the importance of this protease and the results in the experimental section, we performed flexible docking to explore binding interactions of **7-SC2** with the active site of caspase-3 (Fig. 11), and the results showed a strong affinity with binding energy of −8.0 kcal/mol. Considering that the active site of caspase-3 is composed of amino acid residues (TRP206, SER251, ARG64, GLN161, CYS163, SER205, SER120, HIS121, TYR204, SER209, ASN208, TRP214, PHE250, SER249, PHE252, ALA162, SER198 and LEU119), it was found that compound **7-SC2** comprises a set of hydrophobic interactions that potentially confer stability during the binding event, two hydrogens bonds (SER251, ARG64 and GLN161 residues), and four π-interactions between aromatic rings on **7-SC2** and TRP206, ARG207 and CYS163 residues of caspase-3. These findings are consistent with our in vitro results and suggest that hybrid **7-SC2** could be a potential anticancer agent against CRC.

IL-6 is a pleiotropic cytokine that regulates hematopoiesis, inflammation and the immune system. Several recent studies have suggested a potential role for IL-6 in colon cancer initiation and progression, showing that serum levels of IL-6 are elevated in patients with CRC (Zeng et al. 2017). To further explain the experimental results of styrylcoumarin **7-SC2** in the modulation of inflammatory cytokine levels, here we describe computational analysis of the interactions between **7-SC2** and the IL-6 receptor (PDB:

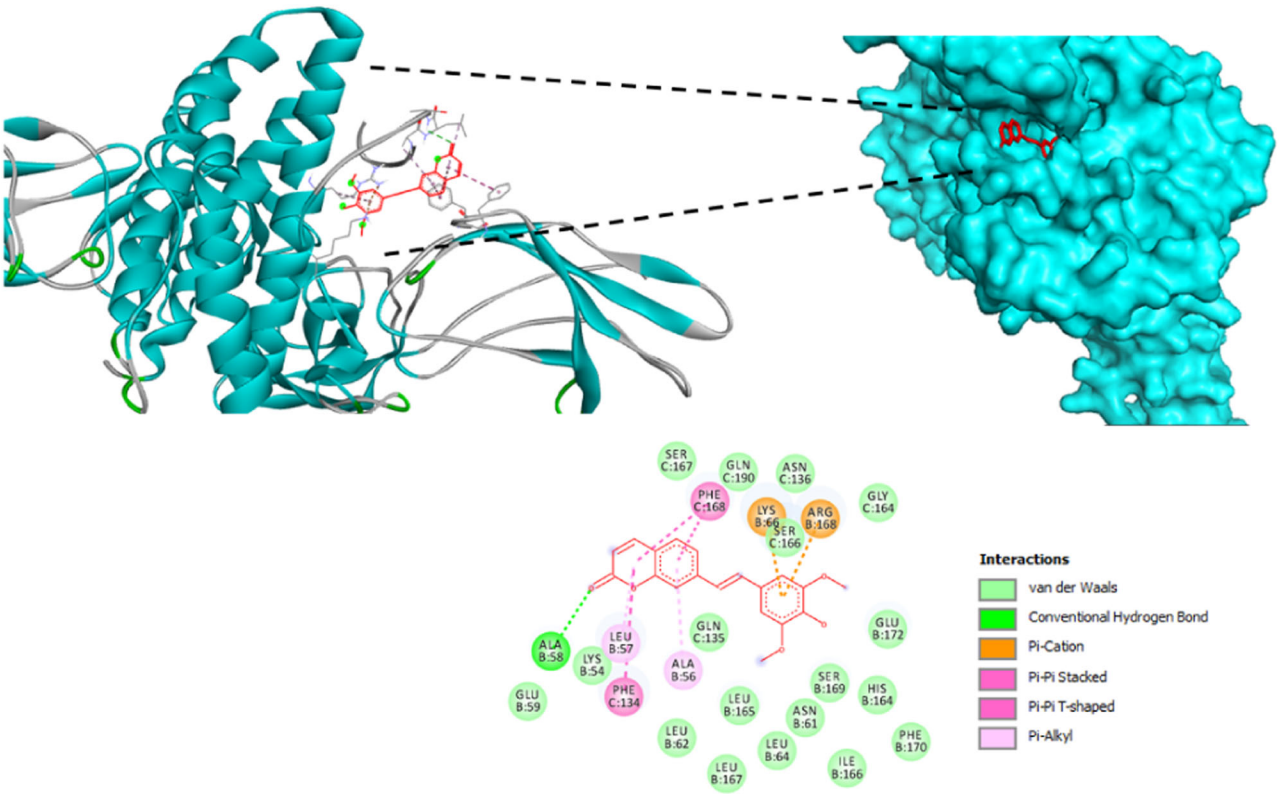

Fig. 12 Binding interactions of styrylcoumarin **7-SC2** at the active site of interleukin-6 (PDB: 1P9M)

1P9M). In the present study, the active site of IL-6 was predicted with higher precision using the metapocket server. This pocket is characterized by the presence of amino acid residues: SER167, GLN190, ASN136, PHE168, LYS166, ARG168, GLY164, ALA58, LEU57, ALA56, PHE134, GLU172 and LEU165. We used this as a starting point for an in silico modeling study. The docking results of hybrid **7-SC2** with IL-6 suggest that it has a good binding affinity (binding energy of –7.7 kcal/mol). On the other hand, the interaction of this compound is through hydrogen bond with ALA58 and produces several Van der Waals interactions with SER166, GLN135, GLY164, LEU165, SER169 and LYS54. Moreover, π-interactions are seen between the aromatic moieties on **7-SC2** and multiple residues such as PHE134, PHE168, LYS66, ARG168, LEU57 and ALA56 (Fig. 12). According to the experimental and docking results, IL-6 could be a potential therapeutic target for styrylcoumarin **7-SC2** and could act as a starting point for clinically useful agents against CRC.

Further docking studies were undertaken to calculate binding energy scoring function of styrylcoumarin **7-SC2** against other types of inflammatory cytokines (COX-2, TNFα and IL-1β) and proteins (MDM2, PARP, Bcl-2, BAX, and VEGF). The results of docking between the ligand and the receptors are shown in Table 2. The highest negative energy value obtained after docking was found between **7-SC2** with the PARP protein, with a value of −10 kcal/mol, followed by **7-SC2** with COX-2, TNFα, MDM2, Bcl-2, VEGF, BAX and IL-1β, with docking scores of −9.3, −7.7, −7.7, −7.6, −7.4, −7.2 and −6.7 kcal/mol, respectively. The interaction between MDM2 and p53 has received a huge attention from scientists due to the important role in the induction of apoptosis and cancer cell survival. The p53–MDM2 interaction surface has been intensively investigated. Fourteen amino acids form a deep hydrophobic cavity on the binding site of p53 in MDM2: LEU54, LEU57, ILE61, MET62, TYR67, GLN72, VAL75, PHE86, PHE91, VAL93, HIS96, ILE99, TYR100 and ILE101 (Kussie et al. 1996). We explored the binding interactions of **7-SC2** with the MDM2 receptor (PDB: 4HG7) in that domain. We found that compound **7-SC2** exhibited the same binding energy than the current inhibitor Nutlin-3a (both 7.7 kcal/mol). This result provides an excellent opportunity to develop small-molecule inhibitors based on **7-SC2** in order to disrupt the p53–Mdm2 interaction. On the other hand, we found that hybrid **7-SC2** has a strong interaction with the apoptotic protein PARP with a docking score of 10 kcal/mol compared with the current drug Talazoparib (11 kcal/mol); however, this result was not consistent with experimental findings, where this compound did not exhibit a significant effect on this protein. We also investigated in silico interactions between

styrylcoumarin **7-SC2** and COX-2. Interestingly, when **7-SC2** was docked into the active site of this cytokine (PDB: 3LN1), it showed a slightly higher binding affinity than the typical drug celecoxib (−9.3 and 9.2 kcal/mol, respectively). This leads to the conclusion that styrylcoumarin **7-SC2** could be a potential inhibitor of COX-2 involved in colon cancer.

Conclusion

We showed that styrylcoumarin **7-SC2** induces apoptosis in SW480 cells, evidenced by the increase in caspase-3, probably by modulation of tumor-suppressor protein p53. Besides, the activation of death signal induced by this hybrid seems to be related with an extrinsic pathway, enhanced by the production of ROS from different sources not associated with mitochondria. In addition, the chemopreventive effect of this hybrid could probably be related with an anti-inflammatory process mediated by the regulation of cytokines such as IL-6. Furthermore, we showed for the first time in vivo experimental evidence that demonstrates the ability of styrylcoumarin **7-SC2** to induce cell death and to inhibit the progression of colon carcinogenesis in the early stage. On the other hand, complementing the experimental findings, the physicochemical and ADME profile of this molecule showed that it has good drug-like properties and thus, it could be a potential active candidate as an oral agent. Besides, styrylcoumarin **7-SC2** exhibited interaction with several apoptotic proteins and anti-inflammatory cytokines such as mutant p53, caspase-3 and IL-6, suggesting that they could be important therapeutic targets for this hybrid compound. Our findings suggest that this compound could be a promising chemopreventive agent against CRC, and thus it is necessary to carry out further studies to elucidate the exact molecular mechanism of action of this hybrid.

Acknowledgements We thank the University of Antioquia (grant CODI 2014-808) for financial support.

Compliance with ethical standards

Conflict of interest The authors declare that they have no conflict of interest.

Publisher's note Springer Nature remains neutral with regard to jurisdictional claims in published maps and institutional affiliations.

References

Alotaibi MR, Hassan ZK, Al-Rejaie SS, Alshammari MA, Almutairi MM, Alhoshani AR, Alanazi WA, Hafez MM, Al-Shabanah OA (2018) Characterization of apoptosis in a breast cancer cell line after IL-10 silencing. Asian Pac J Cancer Prev 19:777–783

Alrawi SJ, Schiff M, Carroll RE, Dayton M, Gibbs JF, Kulavlat M, Tan D, Berman K, Stoler DL, Anderson GR (2006) Aberrant crypt foci. Anticancer Res 26(1A):107–119

Anand P, Kunnumakkara AB, Sundaram C, Harikumar KB, Tharakan ST, Lai OS, Sung B, Aggarwal BB (2008) Cancer is a preventable disease that requires major lifestyle changes. Pharm Res 25:2097–2116

Banki K, Hutter E, Gonchoroff NJ, Perl A (1999) Elevation of mitochondrial transmembrane potential and reactive oxygen intermediate levels are early events and occur independently from activation of caspases in Fas signaling. J Immunol 162:1466–1479

Bellina F, Guazzelli N, Lessi M, Manzini C (2015) Imidazole analogues of resveratrol: synthesis and cancer cell growth evaluation. Tetrahedron 71:2298–2305

Belluti F, Fontana G, Dal Bo L, Carenini N, Giommarelli C, Zunino F (2010) Design, synthesis and anticancer activities of stilbene-coumarin hybrid compounds: Identification of novel proapoptotic agents. Bioorg Med Chem 18:3543–3550

Bird RP, Good CK (2000) The significance of aberrant crypt foci in understanding the pathogenesis of colon cancer. Toxicol Lett 112–113:395–402

Bousserouel S, Lamy V, Gossé F, Lobstein A, Marescaux J, Raul F (2011) Early modulation of gene expression used as a biomarker for chemoprevention in a preclinical model of colon carcinogenesis. Pathol Int 61:80–87

Brentnall M, Rodriguez-Menocal L, De Guevara RL, Cepero E, Boise LH (2013) Caspase-9, caspase-3 and caspase-7 have distinct roles during intrinsic apoptosis. BMC Cell Biol 14:32

Bykov VJ, Wiman KG (2014) Mutant p53 reactivation by small molecules makes its way to the clinic. FEBS Lett 588:2622–2627

Chandrasekaran B, Pal D, Kolluru V, Tyagi A, Baby B, Dahiya NR, Youssef K, Alatassi H, Ankem MK, Sharma AK, Damodaran C (2018) The chemopreventive effect of withaferin A on spontaneous and Inflammationassociated colon carcinogenesis models. Carcinogenesis 39:1537–1547

Corrales-Bernal A, Jaramillo G, Rodríguez B, Kazuz EY, Maldonado-Celis ME (2016) Mango (*Mangifera indica* cv. Azúcar) antiinflammatory and chemopreventive role during colorectal carcinogenesis. Emir J Food Agric 28:704–712

Dash AK, Nayak D, Hussain N, Mintoo MJ, Bano S, Katoch A, Mondhe DM, Goswami A, Mukherjee D (2018) Synthesis and investigation of the role of benzopyran dihydropyrimidinone hybrids in cell proliferation, migration and tumor growth. Anti-cancer Agents Med Chem. https://doi.org/10.2174/1871520618666180903101422.

Ertl P, Rohde B, Selzer P (2000) Fast calculation of molecular polar surface area as a sum of fragment-based contributions and its application to the prediction of drug transport properties. J Med Chem 43:3714–3717

Galizia G, Orditura M, Romano C, Lieto E, Castellano P, Pelosio L, Imperatore V et al. (2002) Prognostic significance of circulating IL-10 and IL–6 serum levels in colon cancer patients undergoing surgery. Clin Immunol 102(2):169–78

García-Gutiérrez N, Maldonado-Celis ME, Rojas-López M, Loarca-Piña GF, Campos-Vega R (2017) The fermented non-digestible fraction of spent coffee grounds induces apoptosis in human colon cancer cells (SW480). J Funct Foods 30:237–246

Gergely Jr P, Niland B, Gonchoroff N, Pullmann Jr R, Phillips PE, Perl A (2002) Persistent mitochondrial hyperpolarization, increased reactive oxygen intermediate production, and cytoplasmic alkalinization characterize altered IL-10 signaling in patients with systemic lupus erythematosus. J Immunol 169:1092–1101

Globocan (2018) http://gco.iarc.fr/today/data/factsheets/populations/170-colombia-fact-sheets.pdf. Accessed 10 Jan 2019.

Hanahan D, Weinberg RA (2011) Hallmarks of cancer: the next generation. Cell 144:646–674

Herrera-R A, Castrillón W, Otero E, Ruiz E, Carda M, Agut R, Naranjo T, Moreno G, Maldonado ME, Cardona-G W (2018) Synthesis and antiproliferative activity of 3- and 7-styrylcoumarins. Med Chem Res 27:1893–1905

Horst JA, Laurenzi A, Bernard B, Samudrala R (2012) Computational multitarget drug discovery. In: Peters J-U (ed.), Polypharmacology in drug discovery. Wiley, Hoboken, NJ, USA, p 263–301

Huang B (2009) MetaPocket: a meta approach to improve protein ligand binding site prediction. OMICS J Integr Biol 3:325–330

Kauntz H, Bousserouel S, Gosse F, Marescaux J, Raul F (2012) Silibinin, a natural flavonoid, modulates the early expression of chemoprevention biomarkers in a preclinical model of colon carcinogenesis. Int J Oncol 41:849–854

Kerru N, Singh P, Koorbanally N, Raj R, Kumar V (2017) Recent advances (2015–2016) in anticancer hybrids. Eur J Med Chem 142:179–212

Knüpfer H, Preiss R (2009) Serum interleukin-6 levels in colorectal cancer patients: a summary of published results. Int J Colorectal Dis 25(2):135–140

Kumar D, Kranthi Raj K, Malhotra SV, Rawat D (2014) Synthesis and anticancer activity evaluation of resveratrol-chalcone conjugates. Med Chem Commun 5:528–535

Kuo GH, Deangelis A, Emanuel S, Wang A, Zhang Y, Connolly PJ, Chen X, Gruninger RH, Rugg C, Fuentes-Pesquera A, Middleton SA, Jolliffe L, Murray WV (2005) Synthesis and identification of [1,3,5] Triazine-pyridine biheteroaryl as a novel series of potent cyclin-dependent kinase inhibitors. J Med Chem 48:4535–4546

Kussie P, Gorina S, Marechal V, Elenbaas B, Moreau J, Levine AJ, Pavletich N (1996) Structure of the MDM2 oncoprotein bound to the p53 tumor suppressor transactivation domain. Science 274:948–953

Li S, Zhang W, Yang Y, Ma T, Guo J, Wang S, Yu W, Kong L (2016) Discovery of oral-available resveratrol-caffeic acid based hybrids inhibiting acetylated and phosphorylated STAT3 protein. Eur J Med Chem 124:1006–1018

Lipinski CA, Lombardo F, Dominy BW, Feeney PJ (2001) Experimental and computational approaches to estimate solubility and permeability in drug discovery and development settings. Adv Drug Deliv Rev 46:3–26

Malami I, Muhammad A, Etti I, Wazirid P, Alhassana A (2017) An in silico approach in predicting the possible mechanism involving restoration of wild-type p53 functions by small molecular weight compounds in tumor cells expressing r273h mutant p53. EXCLI J 16:1276–1287

Maldonado-Celis ME, Roussia S, Foltzer-Jourdainne C, Gossé F, Lobstein A, Habold C, Roessner A, Schneider-Stock R, Raul F (2008) Modulation by polyamines of apoptotic pathways triggered by procyanidins in human metastatic SW620 cells. Cell Mol Life Sci 65:1425–1434

Massagué J (2004) G1 cell-cycle control and cancer. Nature 432:298–306

Mayur YC, Peters GJ, Prasad VV, Lemo C, Sathish NK (2009) Design of new drug molecules to be used in reversing multidrug resistence in cancer cells. Curr Cancer Drug Targets 9:298–306

McQuade RM, Bornstein JC, Nurgali K (2014) Anti-colorectal cancer chemotherapy-induced diarrhoea: current treatments and side effects. Int J Clin Med 5:393–406

Meunier B (2008) Hybrid molecules with a dual mode of action: dream or reality? Acc Chem Res 41:69–77

Morris GM, Goodshell DS, Halliday RS, Huey R, Hart WE, Belew RK, Olson AJ (1998) Docking using a Lamarckian genetic algorithm and empirical binding free energy function. J Comput Chem 19:1639–1662

Morris GM, Huey R, Lindstrom W, Sanner MF, Belew RK, Goodsell DS, Olson AJ (2009) AutoDock4 and AutoDockTools4: automated docking with selective receptor flexibility. J Comput Chem 30:2785–2791

Nepali K, Sharma S, Sharma M, Bedi PM, Dhar KL (2014) Rational approaches, design strategies, structure activity relationship and mechanistic insights for anticancer hybrids. Eur J Med Chem 22:422–487

Nicoletti I, Migliorati G, Pagliacci MC, Grignani F, Riccardi C (1991) A rapid and simple method for measuring thymocyte apoptosis by propidium iodide staining and flow cytometry. J Immunol Methods 139:271–279

Oparka M, Walczak J, Malinska D, van Oppen LMPE, Szczepanowska J, Koopman WJH, Wieckowski MR (2016) Quantifying ROS levels using CM-H2DCFDA and HyPer. Methods 109:3–11

Park HH (2012) Structural features of caspase-activating complexes. Int J Mol Sci 13:4807–4818

Park MT, Lee SJ (2003) Cell cycle and cancer. J Biochem Mol Biol 36:60–65

Paul K, Bindal S, Luxami V (2013) Synthesis of new conjugated coumarin-benzimidazole hybrids and their anticancer activity. Bioorg Med Chem Lett 23:3667–3672

Pérez JM, Maldonado ME, Rojano BA, Alzate F, Sáez J, Cardona W (2014) Comparative antioxidant, antiproliferative and apoptotic effects of ilex laurina and ilex paraguariensis on colon cancer cells. Trop J Pharm Res 13:1279–1286

Phaniendra A, Jestadi DB, Periyasamy L (2015) Free radicals: properties, sources, targets, and their implication in various diseases. Ind J Clin Biochem 30:11–26

Piao Y, Liu Y, Xie X (2013) Change trends of organ weight background data in Sprague–Dawley rats at different ages. J Toxicol Pathol 26:29–34

Pointet AL, Taieb J (2017) Cáncer de colon. EMC - Tratado De Med 21:1–7

Popgeorgiev N, Jabbour L, Gillet G (2018) Subcellular localization and dynamics of the Bcl-2 family of proteins. Front Cell Dev Biol 6:1–11

Redza-Dutordoir M, Averill-Bates DA (2016) Activation of apoptosis signalling pathways by reactive oxygen species. Biochim Biophys Acta 1863:2977–2992

Risio M, Lipkin M, Candelaresi G, Bertone A, Coverlizza S, Rossini FP (2010) Correlations between rectal mucosa cell proliferation and the clinical and pathological features of nonfamilial neoplasia of the large intestine. Cancer Res 151:1917–1921

Rouhollahi E, Moghadamtousi SZ, Al-Henhena N, Kunasegaran T, Hasanpourghadi M, Looi CY, Malek SN, Awang K, Abdulla MA, Mohamed Z (2015) The chemopreventive potential of *Curcuma purpurascens* rhizome in reducing azoxymethaneinduced aberrant crypt foci in rats. Drug Des Dev Ther 9:3911–3922

Russo GL (2007) Ins and outs of dietary phytochemicals in cancer chemoprevention. Biochem Pharm 74:533–544

Saki E, Yazan LS, Ali RMo, Ahmad Z (2017) Chemopreventive effects of germinated rough rice crude extract in inhibiting azoxymethane-induced aberrant crypt foci formation in Sprague–Dawley rats. Biomed Res Int 2017:9517287

Sánchez R, Arboleda G (2008) Mitocondria y muerte celular. NOVA 6:101–236

Sashidhara KV, Kumar A, Kumar M, Sarkar J, Sinha S (2010) Synthesis and in vitro evaluation of novel coumarin-chalcone hybrids as potential anticancer agents. Bioorg Med Chem Lett 20:7205–7211

Selivanova G, Wiman KG (2007) Reactivation of mutant p53: molecular mechanisms and therapeutic potential. Oncogene 26:2243–2254

Sharma R, Zucknick M, London R, Kacevska M, Liddle C, Clarke SJ (2008) Systemic inflammatory response predicts prognosis in patients with advanced-stage colorectal cancer. Clin Colorectal Cancer 7(5 Sep):331–337

Shaveta SM, Singh P (2016) Hybrid molecules: the privileged scaffolds for various pharmaceuticals. Eur J Med Chem 124:500–536

Shen W, Mao J, Sun J, Sun M, Zhang C (2013) Synthesis and biological evaluation of resveratrol-coumarin hybrid compounds as potential antitumor agents. Med Chem Res 22:1630–1640

Shimizu Y, Furuya H, Tamashiro PM, Iino K, Chan OTM, Goodison S, Pagano I, Hokutan K, Peres R, Loo LWM, Hernandez B, Naing A, Chong CDK, Rosser CJ, Kawamori T (2018) Genetic deletion of sphingosine kinase 1 suppresses mouse breast tumor development in an HER2 transgenic model. Carcinogenesis 39:47–55

Sithara T, Arun KB, Syama HP, Reshmitha TR, Nisha P (2017) Morin inhibits proliferation of SW480 colorectal cancer cells by inducing apoptosis mediated by reactive oxygen species formation and uncoupling of Warburg effect. Front Pharmacol 8:640

Steward WP, Brown K (2013) Cancer chemoprevention: a rapidly evolving field. Br J Cancer 109:1–7

Tanaka T (2009) Colorectal carcinogenesis: review of human and experimental animal studies. J Carcinog 8:5

Terzic J, Karin E, Karin M (2010) Inflammation and Colon Cancer. Gastroenterology 2010:2101–2114

Trott O, Olson AJ (2010) AutoDock Vina: improving the speed and accuracy of docking with a new scoring function, efficient optimization, and multithreading. J Comput Chem 3:455–461

Tsogoeva SB (2010) Recent progress in the development of synthetic hybrids of natural or unnatural bioactive compounds for medicinal chemistry. Mini Rev Med Chem 10:773–793

Van Opdenbosch N, Lamkanfi M (2019) Caspases in cell death, inflammation, and disease. Immunity 50(18):1352–1364

Wargovich MJ, Brown VR, Morris J (2010) Aberrant crypt foci: the case for inclusion as a biomarker for colon cancer. Cancers 2:1705–1716

Wargovich MJ, Brown VR, Morris J (2010) Aberrant crypt foci: the case for inclusion as a biomarker for colon cancer. Cancers 2:1705–1716

Westbrook AM, Wei B, Braun J, Schiestl RH (2009) Intestinal mucosal inflammation leads to systemic genotoxicity in mice. Cancer Res 69(11):4827–4834

Xie S, Wang Q, Wu H, Cogswell J, Lu L, Jhanwar-Uniyal M, Dai W (2001) Reactive oxygen species-induced phosphorylation of p53 on serine 20 is mediated in part by Polo-like kinase-3. J Biol Chem 276:36194–36199

Yang J, Liu GY, Dai F, Cao XY, Kang YF, Hu LM, Tang JJ, Li XZ, Li Y, Jin XL, Zhou B (2011) Synthesis and biological evaluation of hydroxylated 3-phenylcoumarins as antioxidants and antiproliferative agents. Bioorg Med Chem Lett 21:6420–6425

Yang N, Hinner M (2002) Getting across the cell membrane: an overview for small molecules, peptides, and proteins. Methods Mol Biol 1266:29–53

Zeng J, Tang Z, Liu S, Guo S (2017) Clinicopathological significance of overexpression of interleukin–6in colorectal cancer. World J Gastroenterol 2017 23:1780–1786